

# INFLUENCE OF FRUIT SHELL PARTICULATE ADDITION ON THE MECHANICAL PROPERTIES, WATER ABSORPTION AND BIODEGRADABILITY OF NATURAL FIBER BASED COMPOSITES

BICHU BABU,\* BENSAM RAJ JESURETNAM,\*\* KALAIYARASAN ANBALAGAN\*\* and  
SIVAPRAKASH MUTHUKRISHNAN\*\*\*

\*Department of Mechanical Engineering, Anna University, Chennai, Tamilnadu - 600025, India

\*\*Department of Mechanical Engineering, Muthayammal Engineering College,  
Rasipuram, Tamilnadu - 637408, India

\*\*\*Department of Mechanical Engineering, Stella Mary's College of Engineering, Nagercoil, Tamilnadu -  
629202, India

✉ Corresponding author: B. Babu, bichubabuphd@gmail.com

Received May 8, 2024

Natural composites are increasingly attracting attention for industrial applications due to their lightweight properties. This study focuses on the development of a novel composite incorporating natural fiber and fruit shell particulates. The composites were prepared using *Terminalia catappa* fiber (IAF) and fruit shell particulates (SP) derived from Indian almond through the traditional hand lay-up technique. The effects of shell particulates on the physical properties of the composites were examined. Four composite variants were fabricated: S0 (Epoxy/IAF), S1 (Epoxy/IAF/3 vol% SP), S2 (Epoxy/IAF/6 vol% SP), and S3 (Epoxy/IAF/9 vol% SP). Tests were conducted to evaluate the tensile, flexural, impact strength, and hardness, as well as water absorption and biodegradability properties of the developed composites. Findings indicated that S3 composites exhibited superior strength due to the incorporation of SP. Additionally, the same composites demonstrated the lowest moisture absorption and degradation rates, attributed to the reinforcing effects of SP. Consequently, the S3 composite appears to be a suitable candidate for structural, automotive, and construction applications.

**Keywords:** natural fiber, natural composites, Indian almond fiber, Indian almond fruit shell, physical properties

## INTRODUCTION

Natural composites have garnered significant attention from researchers and industries due to their desirable properties, including biodegradability, low cost, and lightweight nature. Typically, these composites are derived from natural resources, such as plant products, agricultural waste, and animal-derived materials.

Agricultural wastes are by-products generated during routine agricultural activities, comprising materials such as damaged crops, spoiled fruits, animal waste, processing residues, such as fruit peel and pulp, rice husk, wheat straw *etc.* These wastes are often discarded, without any further utilization or a structured disposal process. Indian almond fruit is one such agricultural waste, produced by the Indian almond tree, as the fruit matures and falls. Although the fruit is edible, it is

less preferred by humans compared to popular fruits like mango, banana, and guava. As a result, it is frequently discarded as waste, alongside other agricultural residues. Converting this fruit waste into value-added products represents a promising opportunity for effective waste management.

The Indian almond fruit contains a single nut surrounded by fibrous material.<sup>1</sup> Some researchers have explored the potential of Indian almond fiber for composite material development, yielding encouraging results. For instance, Nampoohiti *et al.* studied Indian almond/kenaf composites, reporting that three-layer composites with kenaf fiber as the outer layer and Indian almond fiber at the core exhibited high strength. Conversely, composites with Indian almond fiber as the outer layer and kenaf at the core achieved

superior impact strength, but displayed increased degradation and water absorption properties.<sup>2</sup> Natarajan *et al.* investigated the mechanical performance of composites reinforced with Indian almond fiber and silica nanoparticles. The study reported that incorporating 2 wt% silica into Indian almond fiber composite resulted in improved strength and shore D hardness. Additionally, the composite without silica particles exhibited higher moisture absorption than its silica-reinforced counterpart.<sup>3</sup> Sundararaju Perinbakannan *et al.* fabricated Indian almond/banana fiber composites and evaluated their properties. Composites made with four layers of Indian almond fiber demonstrated superior mechanical performance compared to those made with four layers of banana fiber. Furthermore, banana fiber-based composites showed greater mass loss during biodegradation studies.<sup>4</sup>

Existing literature indicates that, while some research has been conducted on Indian almond composites, the potential of Indian almond fruit shells in composite fabrication remains unexplored. Typically, fruit shells can be converted into particulates for use as reinforcement in composite manufacturing. For instance, Pradhan *et al.* developed composites for tribological applications using *Pistacia vera* nutshell particulates, demonstrating that 20 wt% particulate loading yielded optimal abrasive resistance.<sup>5</sup> Similarly, Shravanabelagola Nagaraja Setty *et al.* examined vinyl ester composites reinforced with *Limonia acidissima* shell powder, comparing NaOH-treated and untreated powders. Results revealed that treated powder composites exhibited superior properties, with the maximum performance achieved at a powder loading of 15 wt%.<sup>6</sup>

Seth *et al.* developed composites incorporating Doum palm shell particles and analyzed their tensile and flexural properties. The composite fabricated with 150  $\mu\text{m}$  particles at 10 wt% loading exhibited a tensile strength of 44 MPa, while the composite with 300  $\mu\text{m}$  particles at the same loading demonstrated a tensile strength of 39 MPa. Additionally, the flexural strength of the composite increased from 37 MPa to 57 MPa and 49 MPa for 150  $\mu\text{m}$  and 300  $\mu\text{m}$  particles, respectively, at 10 wt% loading.<sup>7</sup> Durowaye *et al.* investigated the performance of polyester composites reinforced with palm fruit and coconut particulates. The study reported tensile

strengths of 70 MPa for coconut particulate composites and 62.5 MPa for palm fruit particulate composites. Coconut particulates reinforced composites also achieved a higher impact strength, of 4.7 J, compared to 4.6 J for palm fruit particulates. Hardness tests indicated values of 208 BHN and 182 BHN for composites reinforced with coconut and palm fruit particulates, respectively.<sup>8</sup>

Our overview of literature highlights the potential of utilizing fruit shell particulates as reinforcing agent in composite production. This study, therefore, focuses on fabricating natural composites using Indian almond fiber and fruit shell particulates. The research aims to develop a novel lightweight material derived from agricultural waste and to evaluate its physical properties.

## EXPERIMENTAL

### Materials

In this study, composite materials were developed using epoxy as the matrix, and Indian almond fibers and fruit shell particles as reinforcing agents. The fibers were extracted from Indian almond fruits collected locally. Fruit shells of Indian almond were processed into particulates. Epoxy resin (LY556), a hardener (HY951), and a silica release gel were used for composite preparation. The characteristics of Indian almond fiber are presented in Table 1.

### Preparation of fiber and shell particulates

Indian almond fruit consists of flesh, fibers, and an inner shell. The fibers and flesh were separated after immersing the fruit in water for three days. The fibers were manually extracted from the soaked fruit and dried under direct sunlight for one day. Subsequently, a 5% NaOH solution was applied to remove sand, dust, and other impurities from the fiber surface. The dried fruit shells were ground to a particle size of 60 mesh (0.25 mm). The moisture content of the particulates was eliminated by heating them in an oven at 110 °C for 2 h.

### Composite manufacturing

The conventional hand lay-up technique was employed to fabricate composites using epoxy resin, Indian almond fiber, and Indian almond fruit shell particulates. Figure 1 presents photographs of the fiber, fruit shell, and the composite manufacturing process. The process began with the preparation of a resin-hardener mixture in a 10:1 ratio. The Indian almond fruit shell particulates were added to this mixture and homogenized using a mechanical stirrer at 50 rpm for 10 min. The resulting mixture was applied onto the mold surface coated with the release gel using a brush.

A fiber mat of dimensions 200 mm × 200 mm was placed on the coated surface, followed by another layer of the mixture. This sequence of coating and mat placement was repeated until the required fiber weight percentages, as specified in Table 2, were achieved. A roller was gently applied to the fiber mats during the process to remove entrapped air. The mold was then

closed tightly, and a pressure of 6.131 kPa was applied by placing weights on the assembly. The composite was left to cure in this setup for 24 h. After curing, the composite was demolded and left at room temperature for an additional 24 h. The final material was then cut to the required dimensions for experimental investigations.

Table 1  
Characteristics of Indian almond fiber<sup>1</sup>

Characteristic	Values
Density (g/cm <sup>3</sup> )	1.05
Tensile strength (MPa)	85
Young's modulus (GPa)	4
Cellulose (%)	38
Hemicelluloses (%)	29
Lignin (%)	30

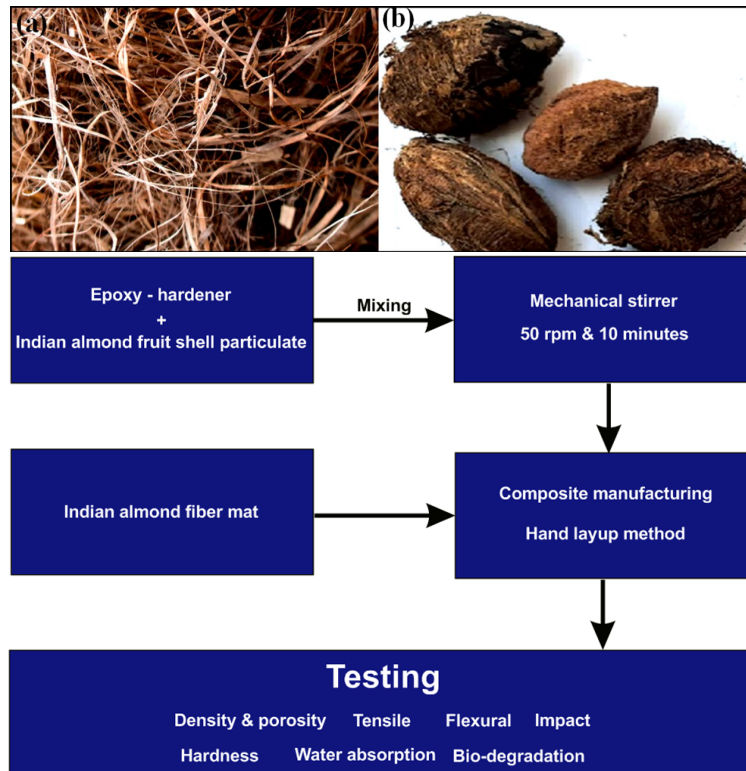


Figure 1: Photographs of (a) Indian almond fiber, and (b) Indian almond fruit shell; (c) Composite manufacturing process

Table 2  
Formulations and denotation of composites

Composite denotation	Epoxy (vol%)	Indian almond fiber (vol%)	Indian almond fruit shell particulates (vol%)
S0	57	43	0
S1	54	43	3
S2	51	43	6
S3	48	43	9

## Experimental works

### Density and porosity determination

The theoretical density of the composites was calculated using Equation (1):

$$\frac{1}{\rho_T} = \frac{W_R}{\rho_R} + \frac{W_M}{\rho_M} \quad (1)$$

where  $\rho_T$  is the theoretical density;  $\rho_R$  is the density of the reinforcement;  $\rho_M$  is the density of the matrix;  $W_R$  is the weight fraction of the reinforcement, and  $W_M$  is the weight fraction of the matrix.

Experimental density was determined through the water immersion test based on Archimedes' principle.<sup>2</sup> Porosity, including closed pores, was calculated using Equation (2):

$$\text{Porosity (\%)} = \frac{(\rho_T - \rho_E)}{\rho_T} \times 100 \quad (2)$$

where  $\rho_E$  is the experimental density.

### Mechanical tests

Tensile and flexural tests were conducted using a universal testing machine (UTM) (Instron 3369). The tensile test was carried out according to ASTM D3039, with a crosshead speed of 5 mm/min. Flexural strength was measured according to ASTM D7264. Impact strength was determined using the IZOD test in accordance with ASTM D256. Shore D microhardness testing was done following ASTM D2240. For each parameter, five specimens were tested, and the average value was considered for analysis. A water uptake test was performed, and the thickness swelling percentage was determined using Equation (3):

$$\text{Thickness swelling (\%)} = \frac{\text{Thickness of wet sample} - \text{Thickness of dry sample}}{\text{Thickness of dry sample}} \times 100 \quad (3)$$

The biodegradability was determined by burying samples in soil maintained at  $30 \pm 2$  °C and  $60 \pm 5\%$  humidity for 60 days. Samples were periodically retrieved, cleaned with distilled water to remove soil residues, and weighed. The percentage mass loss was calculated using Equation (4):

$$\text{Mass loss (\%)} = \frac{\text{Initial mass of sample} - \text{Final mass of sample}}{\text{Final mass of sample}} \times 100 \quad (4)$$

## RESULTS AND DISCUSSION

### Density and porosity of composites

Figure 2 presents the density and porosity characteristics of Epoxy/IAF and Epoxy/IAF/SP composites. A discrepancy between theoretical and experimental densities was observed, attributed to void pressure within the composites.<sup>9</sup> Composite density decreased with increasing SP content, likely due to the lower density of SP

particulates, compared to IAF and epoxy. Consequently, all manufactured composites displayed density values below  $2 \text{ g/cm}^3$ . Among the variants, the S3 composite exhibited the lowest density, while the S0 composite showed the highest. Porosity values were found to increase with higher SP particle content. This behavior could be explained by two factors: (1) the hydrophilic nature of IAF, which absorbed moisture during manufacturing and created voids upon moisture evaporation during curing; and (2) the inclusion of SP particulates increased the contact areas between IAF, SP, and the matrix, leading to more voids. Similar trends have been reported in prior studies.<sup>10,11</sup>

### Tensile strength

Figure 3 depicts the tensile performance of Epoxy/IAF and Epoxy/IAF/SP composites. The tensile strength of the S0 composite, comprising only matrix and IAF, was  $61 \pm 3.04$  MPa. With the inclusion of SP, the strength significantly improved, reaching  $72 \pm 2.32$  MPa for the S3 composite. The enhancement is attributed to improved adhesive strength, better wettability, and fine particulate structure. The tensile strength of S3 was 18% higher than that of S0. Comparable improvements in tensile strength were reported by Dinesh *et al.* and Vijay *et al.*, who observed similar effects from particulate reinforcement.<sup>12,13</sup> Additionally, Dan-Asabe *et al.* demonstrated that 8 wt% banana particulates improved mechanical strength in PVC composites, aligning with findings in this study.<sup>14</sup>

### Flexural strength

The flexural strength results of Epoxy/IAF and Epoxy/IAF/SP composites are presented in Figure 4. The S0 composite demonstrated the lowest flexural strength at  $93 \pm 1.92$  MPa, while the S1, S2, and S3 composites exhibited progressively higher flexural strengths. The incorporation of SP significantly enhanced flexural performance due to the occupation of interfacial spaces between the matrix and IAF, facilitating better load transfer during applied stress. Fallahi *et al.* highlighted that the load transfer efficiency and effectiveness of composites depend on the fiber-matrix interface.<sup>15</sup> The S3 composite achieved the highest flexural strength, recorded at  $118 \pm 2.54$  MPa, which represents a 26.8% improvement compared to the S0 composite. The increase in SP

weight percentage positively influenced the strength, attributed to enhanced interfacial bonding and structural stiffness. Similar findings were reported by Vivek *et al.*, who developed epoxy-based natural composites reinforced with

bagasse ash particulates, noting that the inclusion of ash improved stiffness and bonding strength.<sup>16</sup> These results align with the current study, reinforcing the role of particulates in enhancing flexural properties.

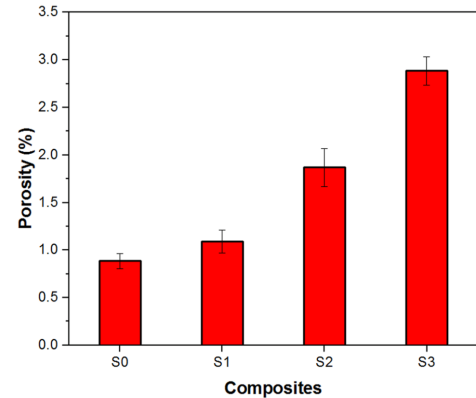
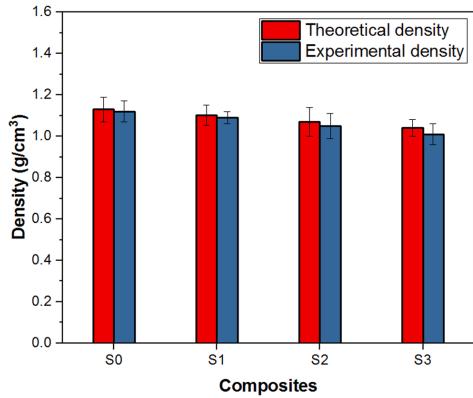


Figure 2: Density (a) and porosity (b) of Epoxy/IAF and Epoxy/IAF-SP composites

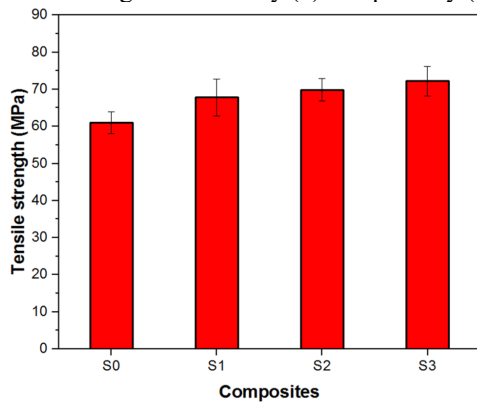


Figure 3: Tensile strength of Epoxy/IAF and Epoxy/IAF-SP composites

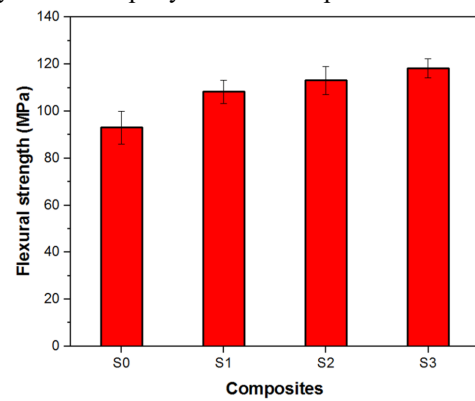


Figure 4: Flexural strength of Epoxy/IAF and Epoxy/IAF-SP composites

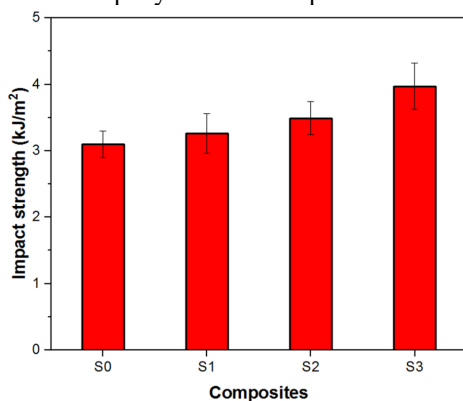


Figure 5: Impact strength of Epoxy/IAF and Epoxy/IAF-SP composites

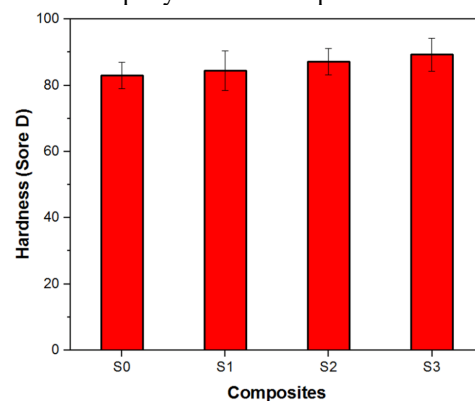


Figure 6: Hardness of Epoxy/IAF and Epoxy/IAF-SP composites

### Impact strength

Figure 5 illustrates the impact strength results of Epoxy/IAF and Epoxy/IAF/SP composites. The S0 composite exhibited the lowest impact strength at  $3.1 \pm 0.45$  kJ/m<sup>2</sup>, while the S3 composite demonstrated the highest impact

strength at  $3.97 \pm 0.61$  kJ/m<sup>2</sup>. The impact strength of S1, S2, and S3 composites exceeded that of the S0 composite, which can be attributed to the reinforcing effect of SP particulates. The SP particulates contributed to improved wettability between the matrix and IAF, facilitating better

stress transfer under impact loading. Saha *et al.* similarly reported that pineapple fiber/pineapple leaf particulate composites benefited from particulates enhancing fiber-matrix wettability, leading to improved bonding strength and load transfer.<sup>17</sup> The improved stress transfer in the current study prevented premature failure of the reinforcement and matrix during impact loading, thereby significantly enhancing the impact strength. Among all composites, S3 exhibited the highest impact strength, demonstrating the effectiveness of SP inclusion in improving mechanical properties.

**Hardness**

The hardness results of Epoxy/IAF and Epoxy/IAF/SP composites are presented in Figure 6. The S0 composite displayed the lowest hardness value of  $83 \pm 0.82$ , which can be attributed to the absence of reinforcing effects. In contrast, S1, S2, and S3 composites exhibited higher hardness values due to the reinforcing role of SP particulates. The SP particulates were uniformly distributed within the matrix, reducing the gaps between the matrix and IAF. This resulted in increased resistance to penetration by the indenter, thereby enhancing the hardness of the composites. Similar findings were reported by Dinesh *et al.*, who observed that the dispersion of wood particles in jute composites resisted penetration and improved hardness.<sup>12</sup> Among the composites, S3 exhibited the highest hardness of  $89 \pm 0.64$ , representing a 7.2% improvement over S0. The increase in SP content from 3 vol% to 9 vol% significantly improved hardness due to the gap-filling effect of SP particulates.

**Water absorption**

Water absorption characteristics of Epoxy/IAF and Epoxy/IAF/SP composites are shown in Figure 7, which plots thickness swelling against time. The hydrophilic nature of IAF led to water absorption, increasing thickness swelling in all composites over time. The S0 composite exhibited the highest thickness swelling due to the exclusive presence of IAF. In S1, S2, and S3 composites, the inclusion of SP particulates reduced the gaps between the matrix and filler, leading to decreased water absorption and thickness swelling. The swelling behavior followed the sequence:  $S1 > S2 > S3$ , indicating that increasing SP content reduced thickness swelling. All composites reached a saturation state after 10 days of immersion, demonstrating stabilized water absorption.

**Biodegradation**

The biodegradability of Epoxy/IAF and Epoxy/IAF/SP composites is depicted in Figure 8. All composites experienced mass loss with increasing burial time due to the natural degradation tendency of the materials. The degradation pattern was linear up to 40 days, after which a steep increase in mass loss was observed. The S0 composite exhibited the highest degradation among all composites, attributed to its higher moisture absorption, which promoted bacterial attack. Conversely, the S3 composite displayed the lowest degradation due to its reduced moisture absorption characteristics. The degradation sequence observed was:  $S0 > S1 > S2 > S3$ , indicating that the inclusion of SP particulates effectively slowed the degradation process.

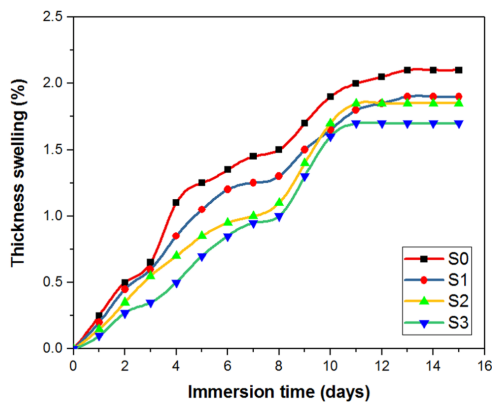


Figure 7: Water absorption characteristics of Epoxy/IAF and Epoxy/IAF-SP composites

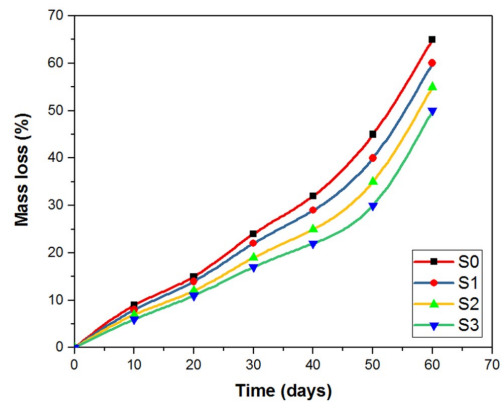


Figure 8: Biodegradation behavior of Epoxy/IAF and Epoxy/IAF-SP composites

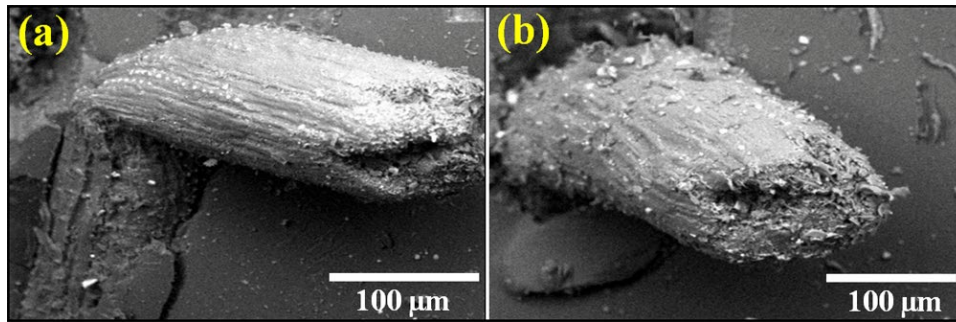


Figure 9: SEM micrographs of tensile fractured samples, (a) S0 and (b) S1

Table 3

Comparison of prepared composite with other composites reinforced with different natural fibers/particles

Materials	Tensile strength (MPa)	Flexural strength (MPa)	Impact strength (kJ/m <sup>2</sup> )	Ref.
Epoxy/IAF/SP	72.2	118.2	3.97	Present study
Epoxy/ <i>Abutilon indicum</i>	64	-	-	[18]
Epoxy/Sugarcane bagasse	45	-	-	[19]
Epoxy/ <i>Moringa oleifera</i> fruit pod particulates	31	37	0.011	[20]
Epoxy/ <i>Cordia dichotoma</i>	63	347	-	[21]
Epoxy/Carbonized coconut shell particles	338.75	156	0.149	[22]
Epoxy/ <i>Dichrostachys cinerea</i>	50	74	-	[23]
Epoxy/ <i>Erythrina variegata</i>	101	108	8.4	[24]

This was likely due to the improved wettability provided by SP particulates, which reduced moisture absorption and degradation.

### SEM analysis

The tensile-fractured samples were analyzed using SEM to study their morphology, as shown in Figure 9. The SEM micrographs revealed fiber pull-out in the S0 sample, while the S1 sample exhibited clear-cut fiber breakage. The weaker adhesive strength in the S0 composite allowed fibers to detach from the resin under loading, whereas the S1 composite demonstrated enhanced bonding strength between the fiber, matrix, and SP particulates, preventing fiber pull-out. This improved bonding in S1 resulted in higher strength compared to S0. The morphological observations were consistent with the experimental findings, reinforcing the role of SP particulates in enhancing composite properties.

### Comparison of performance of manufactured composite with natural composites in literature

The performance of the Epoxy/IAF/SP composite was compared with previously reported natural composites, as detailed in Table

3. The tensile strength of the Epoxy/IAF/SP composite was found to be comparable to that of nylon/empty fruit bunch fiber/coconut shell particulate composite and higher than those of other materials, such as polypropylene/Doum palm shell particles, vinyl ester/*Limonia acidissima* shell powder, epoxy/*Moringa oleifera* fruit pod particulates, polyester-African star apple shell powder-waste toner powder, polyester/palm kernel shell particles and polyethylene/*Tetracarpidium conophorum* shell particulates. However, it exhibited lower tensile strength compared to the epoxy/carbonized coconut shell particle composite. For flexural strength, the Epoxy/IAF/SP composite showed superior performance compared to polypropylene/Doum palm shell particles, epoxy/*Moringa oleifera* fruit pod particulates, and polyester-African star apple shell powder-waste toner powder composites, and exhibited lower values than vinyl ester/*Limonia acidissima* shell powder and epoxy/carbonized coconut shell particles composites. In terms of impact strength, the Epoxy/IAF/SP composite outperformed the nylon/empty fruit bunch fiber/coconut shell particles composite, but showed lower values

compared to vinyl ester/*Limonia acidissima* shell powder, epoxy/*Moringa oleifera* fruit pod particulates, and epoxy/carbonized coconut shell particles composites. Overall, the performance of the Epoxy/IAF/SP composite aligns well with the trends reported in the literature, demonstrating its competitiveness and potential as a sustainable material for various applications.

## CONCLUSION

This study investigated the properties of composites made with Indian almond fiber (IAF) and Indian almond fruit shell particulates (SP). The tensile tests demonstrated that the S3 composite (Epoxy/IAF/9 vol% SP) achieved the highest tensile strength (72 MPa), attributed to improved adhesion between the matrix, fiber, and filler. The S3 composite also exhibited superior flexural strength (118 MPa) due to enhanced load transfer within the matrix and reinforcements. Additionally, the highest impact strength of 3.97 kJ/m<sup>2</sup> was recorded for the same composite. Shore D hardness testing revealed that the S3 composite had the highest hardness value (89), indicating improved surface resistance. Water absorption and biodegradation studies showed that the S0 composite absorbed more moisture and degraded more rapidly, while the S3 composite exhibited reduced water absorption and slower mass loss. This behavior was attributed to the reinforcing effect of SP particulates, which improved the composite's resistance to moisture and microbial degradation.

## REFERENCES

- <sup>1</sup> J. Jeyaraman, B. R. Jesuretnam and K. Ramar, *J. Nat. Fibers*, **19**, 4381 (2022), <https://doi.org/10.1080/15440478.2020.1858219>
- <sup>2</sup> E. N. Nampoothiri, J. Bensam Raj, R. Thanigaivelan and R. Karuppasamy, *J. Nat. Fibers*, **19**, 292 (2022), <https://doi.org/10.1080/15440478.2020.1739592>
- <sup>3</sup> S. Natarajan, G. Pathinettampadian, M. Vadivel, P. S. S. Yesudasan and B. R. Jesuretnam, *J. Nat. Fibers*, **19**, 12004 (2022), <https://doi.org/10.1080/15440478.2022.2048942>
- <sup>4</sup> A. Sundararaju Perinbakannan, M. Karuppusamy and K. Ramar, *J. Nat. Fibers*, **19**, 7049 (2022), <https://doi.org/10.1080/15440478.2021.1941489>
- <sup>5</sup> S. Pradhan, V. Prakash and S. K. Acharya, *J. Mater. Des. Appl.*, **236**, 334 (2022), <https://doi.org/10.1177/14644207211044716>
- <sup>6</sup> V. K. Shravanabelagola Nagaraja Setty, G. Govardhan, S. Mavinkere Rangappa and S. Siengchin,

- J. Vinyl Addit. Technol.*, **27**, 97 (2021), <https://doi.org/10.1002/vnl.21787>
- <sup>7</sup> S. A. Seth, I. S. Aji and A. Tokan, *Int. J. Sci. Res. Eng. Tech.*, **7**, 645 (2018)
- <sup>8</sup> S. I. Durowaye, G. I. Lawal, M. A. Akande and V. O. Durowaye, *Int. J. Mater. Eng.*, **4**, 141 (2014), <https://doi.org/10.5923/j.ijme.20140404.04>
- <sup>9</sup> A. Saha, S. Kumar and A. Kumar, *J. Polym. Res.*, **28**, 1 (2021), <https://doi.org/10.1007/s10965-021-02435-y>
- <sup>10</sup> A. Satapathy, A. K. Jha, S. Mantry, S. K. Singh and A. Patnaik, *J. Reinf. Plast. Compos.*, **29**, 2869 (2010), <https://doi.org/10.1177/0731684409341757>
- <sup>11</sup> B. Madsen and H. Lilholt, *Compos. Sci. Technol.*, **63**, 1265 (2003), [https://doi.org/10.1016/S0266-3538\(03\)00097-6](https://doi.org/10.1016/S0266-3538(03)00097-6)
- <sup>12</sup> S. Dinesh, P. Kumaran, S. Mohanamurugan, R. Vijay, D. L. Singaravelu *et al.*, *J. Polym. Res.*, **27**, 1 (2020), <https://doi.org/10.1007/s10965-019-1975-2>
- <sup>13</sup> R. Vijay, A. Vinod, R. Kathiravan, S. Siengchin and D. L. Singaravelu, *J. Ind. Text.*, **49**, 1252 (2020), <https://doi.org/10.1177/1528083718811086>
- <sup>14</sup> B. Dan-Asabe, *J. King Saud Univ. Eng. Sci.*, **30**, 296 (2018), <https://doi.org/10.1016/j.jksues.2016.11.001>
- <sup>15</sup> H. Fallahi, O. Kaynan and A. Asadi, *Compos. A: Appl. Sci. Manuf.*, **166**, 107390 (2023), <https://doi.org/10.1016/j.compositesa.2022.107390>
- <sup>16</sup> S. Vivek and K. Kanthavel, *Compos. B Eng.*, **160**, 170 (2019), <https://doi.org/10.1016/j.compositesb.2018.10.038>
- <sup>17</sup> A. Saha, S. Kumar and A. Kumar, *J. Polym. Res.*, **28**, 1 (2021), <https://doi.org/10.1007/s10965-021-02435-y>
- <sup>18</sup> D. Mohana Krishnudu, D. Sreeramulu and P. V. Reddy, *J. Nat. Fibers*, **17**, 1775 (2020), <https://doi.org/10.1080/15440478.2019.1598917>
- <sup>19</sup> A. N Balaji and K. J. Nagarajan, *Carbohydr. Polym.*, **174**, 200 (2017), <https://doi.org/10.1016/j.carbpol.2017.06.065>
- <sup>20</sup> I. O. Oladele, G. S. Ogunwande, A. S. Taiwo and S. S. Lephuthing, *Heliyon*, **8**, 09755 (2022), <https://doi.org/10.1016/j.heliyon.2022.e09755>
- <sup>21</sup> B. M. Reddy, Y. V. Mohana Reddy, B. C. Mohan Reddy and R. M. Reddy, *J. Nat. Fibers*, **17**, 759 (2020), <https://doi.org/10.1080/15440478.2018.1534183>
- <sup>22</sup> J. O. Agunsoye, A. K. Odumosu and O. Dada, *J. Adv. Manuf. Technol.*, **102**, 893 (2019), <https://doi.org/10.1007/s00170-018-3206-0>
- <sup>23</sup> T. H. Nam, S. Ogihara, N. H. Tung and S. Kobayashi, *Compos. B: Eng.*, **42**, 1648 (2011), <https://doi.org/10.1016/j.compositesb.2011.04.001>
- <sup>24</sup> B. T. Parthasarathi, S. Arunachalam, N. K. Jawaharlal and M. C. R. Balasundaram, *Cellulose Chem. Technol.*, **58**, 349 (2024), <https://doi.org/10.35812/CelluloseChemTechnol.2024.58.34>